Montogue

Quiz HD106

River Hydraulics

Lucas M. Nogueira

PROBLEMS

Problem 1

The downstream hydraulic geometry of rivers can be examined by combining four relationships.

Firstly, under steady-uniform bankfull flow conditions, the dominant discharge Q is

$$Q = WhV \quad \text{(Eq. 1)}$$

where the mean velocity V is normal to the cross-section area, and h is the mean flow depth obtained from the cross-section area divided by the bankfull width W. The width-depth ratio of most rivers is sufficiently large that it may be assumed that the hydraulic radius R_h is approximately equal to h.

Secondly, the power form of the resistance equation is

$$V = a\sqrt{g}\left(\frac{h}{d_s}\right)^m h^{1/2} S^{1/2} \quad \text{(Eq. 2)}$$

where a is a resistance coefficient, g ≈ 9.81 m/s^2, h is river depth, d_s is grain size, S is slope, and m is an exponent given by

$$m = \frac{1}{2.3\log\left(2h/d_{50}\right)}$$

where d_{50} is the median grain diameter. The third equation is the Shields parameter,

$$\tau^* = \frac{hS}{\left(G_s - 1\right)d_s} \quad \text{(Eq. 3)}$$

where G_s is the specific gravity of the bed particles. The critical value of the Shields parameter is $\tau^* \approx 0.047$, which defines the beginning of motion of noncohesive particles in turbulent flows over rough boundaries. Recall that, in the Shields parameter framework, the beginning of motion of noncohesive particles occurs at a threshold value $\tau_c^\star$; beyond this threshold value, sediment transport increases with the Shields number. Lastly, the fourth equation we require is

$$\tan\lambda = b_r\left(\frac{h}{d_s}\right)^{2m}\frac{h}{W} \quad \text{(Eq. 4)}$$

where λ is the deviation angle of streamlines near the bed, and b_r, known as the river-bed coefficient, is a parameter assumed constant and given by

$$b_r = \frac{a^2 W}{\Omega_R R}$$

where R is the radius of curvature and Ω_R is the ratio of the centrifugal force generating secondary motion to the shear force abating the motion and dissipating energy.

Note that the four equations include 13 variables, namely the width W, the depth h, the velocity V, the slope S, the flow rate Q, the sediment diameter d_s, the Shields parameter $\tau^\star$, the deviation angle λ (or, more precisely, its tangent *tan* λ), the gravitational acceleration g, the resistance coefficient a, the constant b_r, the specific gravity G_s, and the exponent m. Deeper analysis into this system of equations has shown that flow Q, sediment diameter d_s, and Shields parameter $\tau^\star$ are the primary independent variables, whereas variability in other parameters is comparatively small. On the basis of these three variables, Julien and Wargadalam (1995) established empirical correlations for the flow depth h, the width W, the velocity V, and the slope S, namely

$$\begin{cases} h \approx 0.133 Q^{\frac{1}{3m+2}} d_{50}^{\frac{6m-1}{6m+4}} \tau_*^{\frac{-1}{6m+4}} \\ W \approx 0.512 Q^{\frac{2m+1}{3m+2}} d_{50}^{\frac{-4m-1}{6m+4}} \tau_*^{\frac{-2m-1}{6m+4}} \\ V \approx 14.7 Q^{\frac{m}{3m+2}} d_{50}^{\frac{2-2m}{6m+4}} \tau_*^{\frac{2m+2}{6m+4}} \\ S \approx 12.4 Q^{\frac{-1}{3m+2}} d_{50}^{\frac{5}{6m+4}} \tau_*^{\frac{6m+5}{6m+4}} \end{cases}$$

where Q is in cubic meters per second, the median grain diameter d_{50} is in meters, and τ^* is expressed as

$$\tau^* = \frac{\gamma h S}{(\gamma_s - \gamma) d_{50}}$$

where γ_s is the specific gravity of soil and γ is the specific gravity of water. Lastly, exponent m is calculated as

$$m = \frac{1}{2.3\log_{10}(2h/d_{50})}$$

Using the relationships presented above and taking Q = 200 m^3/s, d_{50} = 28 mm, and τ^* = 0.05, compute W, V, and S. Assume the Manning-Strickler approximation to be valid.

▶ Problem 2

A meandering river has length 500 m and radius of curvature R_m = 83 m. Compute the maximum deviation angle θ_m, the valley length Λ, the sinuosity Ω, and the meander width W_m.

▶ Problem 3

Regarding various aspects of the theory of river dynamics and hydraulics, true or false?

1.( ) Williams (1978) used data from over 200 American reaches to develop correlations for bank-full discharge. The correlations expressed discharge in terms of three variables that were readily available for most of the surveyed streams, namely cross-sectional area, longitudinal slope, and bank-full depth. Crucially, Williams' correlations expressed discharge as a function of area and slope only; bank-full depth was not included because regression analysis showed that this variable was not statistically significant.

Recommended research: Williams (1978).

The term *hydraulic geometry* connotes the relationships between the mean stream channel form and discharge both at-a-station and downstream along a stream network in a hydrologically homogeneous basin. In the 1950s, Leopold and Maddock (quoted in Singh, 2003) expressed the hydraulic geometry relationships for a channel in the form of power functions based on discharge Q, namely

$$B = aQ^b \;\; ; \;\; d = cQ^f \;\; ; \;\; V = kQ^m$$

where B is the channel width, d is the flow depth, V is the flow velocity, and a, b, d, c, f. k, m are parameters. These equations are complemented by

$$n = NQ^p \;\; ; \;\; S = sQ^y$$

where n is Manning's roughness factor, S is slope, and N, p, s, y are parameters.

2.( ) The equations above have been calibrated for a range of environments. For example, Parker (1979) noted that the exponents b, f and m are highly variable from locality to locality, whereas the scale factors a, d, and k were found to be remarkably unaltered.

Recommended research: Singh (2003); Parker (1979).

3.( ) Yang *et al.* (1981) referred to Leopold and Maddock's power laws and attempted to determine exponents b, f and m on the basis of the theory of minimum rate of energy dissipation. Importantly, the exponents obtained by Yang's team were based on the Chézy equation and applied to trapezoidal channels only.

Recommended research: Yang *et al.* (1981).

Aware of the scarcity of previous efforts, Oueslati *et al.* (2015) used streamflow data in an attempt to classify the hydrological regimes of the Mediterranean's ungauged rivers. Their work included performing a principal component analysis (PCA) starting from no less than 40 hydrologic indices gleaned from the literature, so as to ascertain those that were most representative of the 60 streams – 20 temporary rivers and 40 perennial rivers – included in their study.

4.( ) Crucially, Oueslati's group found that perennial rivers are mainly described by high-flow hydrologic indices, whereas temporary ones are described by indices of duration of no-flow conditions, indices of variability, and indices of predictability. ■ **(A black square indicates the end of a multi-paragraph statement.)**

Recommended research: Oueslati *et al.* (2015).

5.( ) Sternberg's law was introduced in the late 19th century as a means to represent the diminishing size of bed sediment across a stream's longitudinal course. This relationship relies on the so-called fining rate δ, which determines the rate at which sediment size decreases along a stream. This parameter is expected to be greater for, say, a lowland sand-bed river than for, say, a steep mountain torrent.

Researchers have adapted Bagnold's celebrated work on wind-blown sand to the context of sediment transport in rivers. In this modified theory, bedload transport in gravel-bed rivers is assumed to occur at a very low rate up to a certain critical level of streamflow, then to increase at a faster-than-linear rate with flow above this threshold. This threshold can be described in terms of a critical shear stress or a critical stream power. However, the latter is often preferred over the former because it does not require local flow properties to be known. This advantage is defeated, however, if we observe that some critical stream power equations include flow depth as one of the unknowns.

6.( ) Ferguson (2005) used the critical stream power concept in a model of his own. His formulation improves upon Bagnold's theory by including the effects of grain hiding and protrusion on the mobility of different sediment sizes. On the other hand, it still relies on knowledge of local flow properties (depth and velocity) and not just on channel properties such as width and bed gradient, as would be expected of a stream power-based model. ■

Recommended research: Ferguson (2005).

7.( ) Since longitudinal river adjustment progresses in geologic timescales, river morphologists are left with numerical modelling as one of the few tools with which to study these processes. The following table shows the longitudinal profiles expected to result for different combinations of (1) grain size of bed material, d; (2) bankfull discharge, Q_{bk}; and (3) bankfull sediment discharge, Q_{sbk}. x denotes horizontal distance. We can surmise that the missing profile is a 'mildly concave upward' profile such as the one illustrated to the side.

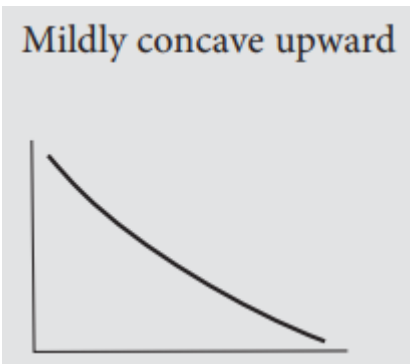

Recommended book: Rhoads (2020).

Sand-bed		Gravel-bed	
$d \propto e^{-0.003x}$ Q_{bk} = const. (~30 m^3/s) Q_{sbk} = const. (~0.0136 m^3/s)	Linear to slightly concave upward 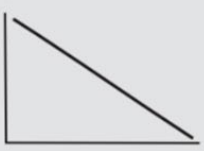	$d \propto e^{-0.02x}$ Q_{bk} = const. (~30 m^3/s) Q_{sbk} = const. (~0.0136 m^3/s)	?
d = const. (~0.4 mm) $Q_{bk} \propto x^{1.2}$ Q_{sbk} = const. (~0.0136 m^3/s)	Strongly concave upward 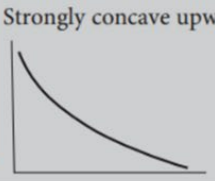	d = const. (~6 mm) $Q_{bk} \propto x^{1.2}$ Q_{sbk} = const. (~0.0136 m^3/s)	Strongly concave upward 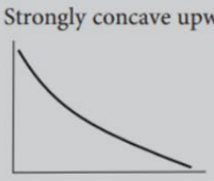
d = const. (~0.4 mm) Q_{bk} = const. (~30 m^3/s) $Q_{sbk} \propto x^{1.2}$	Convex upward 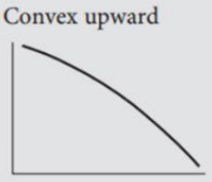	d = const. (~6 mm) Q_{bk} = const. (~30 m^3/s) $Q_{sbk} \propto x^{1.2}$	Convex upward 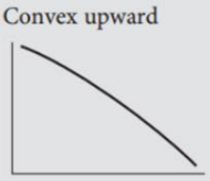

8.( ) Hasegawa (1989) introduced a coefficient for use in the evaluation of bank erosion rates. Noting that this coefficient should be a function of bank soil properties only, Hasegawa went on to show that his novel parameter could be readily associated with data obtained from a cone penetrometer test (CPT) device, preferably one equipped with a geophone.

Recommended research: Hasegawa (1989).

Until recently, few studies had examined the characteristics of large-scale coherent flow structures in natural rivers where beds are very rough. This is due to the difficulty of collecting high-quality turbulence data in these environments. The relationship between large-scale flow structures and eddy shedding must be better understood because vortices downstream of protruding clasts have been implicated as the most significant process by which energy is dissipated within a river flow.

9.( ) Roy *et al.* (2004) elucidated these issues through an investigation on macro-turbulent flow structures in gravel-bed rivers. Their work offers substantial insight not only into large-scale flow structures in gravel-bed streams, but also on the complex dynamics of these structures as they develop and advect downstream on a rough bed. Indeed, their quantitative data allowed for a thorough investigation of momentum exchange associated with the structures; what's more, Roy's model enabled a hydrodynamic analysis of smaller-scale eddies that may play a key role in the development of the large-scale flow structures. ■

Recommended research: Roy *et al.* (2004).

10.( ) Shvidchenko and Pender (2001) studied the turbulent motion of water through an experimental flume overlain by a mobile gravel bed. The following figure illustrates the three-dimensional structures yielded by their experiments. The blue rectangle superposes the longitudinal size of the eddies observed in their experiments, whereas the red square covers the transverse size; h denotes

flow depth. With reference to the results of Shvidchenko and Pender, we can replace the red square with **"6 to 8"** and the blue square with **"2."**

Reference: Shvidchenko and Pender (2001).

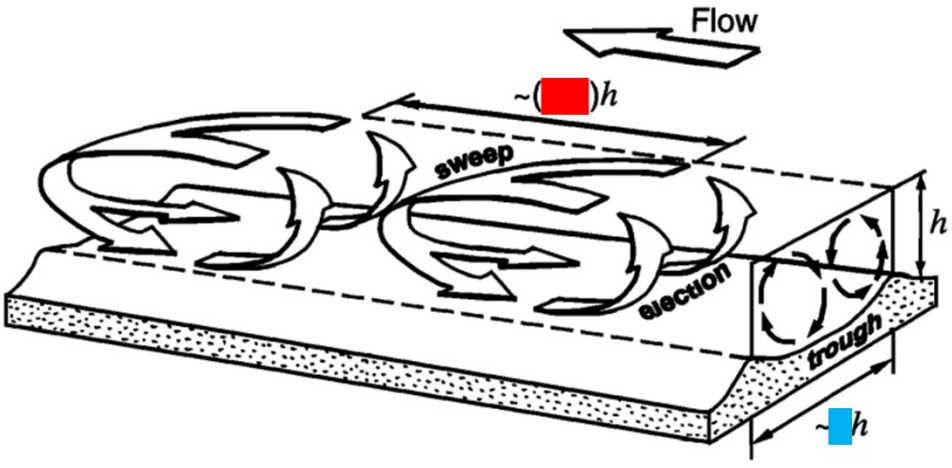

11.( ) MacDonald et al. (2007) performed measurements in the near-field region of the Merrimack River plume in the northeastern USA, aiming to obtain estimates of turbulent kinetic energy dissipation rates. The measurements were then compared with results from a highly resolved three-dimensional model, and good agreement was achieved. One exception, however, was the base of the river plume, wherein MacDonald's team verified substantial disagreement between the measured data and numerical simulation results.

Recommended research: MacDonald *et al.* (2007).

Rodríguez and García (2008) conducted laboratory experiments to assess secondary circulation dynamics in straight open-channel flows with a rough bed. Their study was partially motivated by the rule of thumb, commonly accepted in the literature, that secondary flow patterns in a rectangular channel of width b and height h, if they occur at all, will die out at a distance of $b > 2.5h$ from the walls. Further, it has been posited that secondary circulation may not occur at all at ratios b/h of 5 or less.

12.( ) Rodríguez and his colleague reported results that run counter to these rules of thumb, in that they detected turbulence-induced secondary currents for b/h greater than 5.0. ■

Recommended research: Rodríguez and García (2008).

Research has shown that the variability of bed shear stress in a river reach is associated with the occurrence of large-scale flow structures (LSFS). Franca and Lemmin (2015) used an acoustic Doppler velocity profiler (ADVP) to perform measurements of LSFSs in the Venoge river in Switzerland.

One immediate contribution of their study was that it confirmed the existence of LSFS patterns in a river flow with lower relative submergence (i.e., ratio of flow depth to bed grain diameter) than previously known, thereby extending the applicability of the LSFS concept.

Three-dimensional velocities phase-averaged over one LSFS cycle indicated a large-scale sweep-ejection sequence in phase with the passage of a LSFS in a certain segment of the flow at a given time. Simply put, a 'sweep' is associated with a positive LSFS, whereas an 'ejection' is associated with a negative LSFS.

13. ( ) Importantly, Franca and his colleague noted that compared to ejections, sweeps generally accounted for a shorter fraction of the LSFS life cycle. ■

Recommended research: Franca and Lemmin (2015).

Chen and Duan (2006) proposed an analytical model to simulate width adjustment in meandering channels. Their model is mathematically simple and provides interesting insights into meandering dynamics.

14.( ) One important parameter in the Chen-Duan model is the scour factor A, which characterizes the transverse bed slope. Aiming to establish the sensitivity of model results to this parameter, those workers conducted equivalent simulations for A variable with time and for A fixed at 2.0. Interestingly, they

found that a timewise-variable *A* led to unrealistic results, hence they adopted *A* = 2.0 throughout the demonstrative application of their model. ■

Recommended research: Chen and Duan (2006).

15.( ) The braiding index is the average number of channels along several transects oriented perpendicularly to the river direction within a reach of a given length. In general, the braiding index increases with increasing stream power.

16.( ) Sun *et al.* (1996) conducted a historically important simulation of river meandering. Theirs was a three-dimensional model, with allowance for river topography and compaction of sedimentary materials with large void ratios.

Recommended research: Sun *et al.* (1996).

17.( ) Lancaster and Bras (2002) developed a simple model for realistic river meandering evolution. They found, among other things, that compound bend formation is highly sensitive to both valley slope and grain size.

Recommended research: Lancaster and Bras (2002).

Zinger *et al.* (2011) used a combination of aerial imagery, GPS mapping and measurements of channel bathymetry to quantify the erosional flux of floodplain sediment mobilized by two chute cutoff events on a large meander bend on the Wabash River in the American Midwest. Zinger and her colleagues showed that chute cutoff events may perform geomorphic work at extreme rates, releasing large pulses of sediment into river channels from adjacent floodplains.

18.( ) Indeed, Zinger *et al.* (2011) found that the erosional flux mobilized by the chute cutoff events in question could be as much as five orders of magnitude greater than the sediment fluxes associated with lateral migration of individual bends along the river. ■

Recommended research: Zinger *et al.* (2011).

19.( ) Wrzesinski (2016) notes that quantification of uncertainty in a river basin's runoff regime is an important issue for applications such as water supply and floodplain mapping. Borrowing from Shannon's information theory, Wrzesinski proposed an entropy function for runoff volume, which he went on to apply to Poland's river network. Entropy values ranged from 0.532 to 3.599 bits; particularly high values, indicating high degrees of runoff volume uncertainty, were mostly associated with mountain rivers.

Recommended research: Wrzesinski (2016).

Since most studies of fluvial systems cover relatively short time spans – say, 5 years or so – one of the few sources of data available for long-term research is the historical record. Kondolf *et al.* (2007) exemplified this approach by documenting the historical evolution of lower Eygues River in southeastern France with the aid of 19th-century Napoleanean parcel maps and 20th-century topographic maps and aerial photographs.

20.( ) As reported by Kondolf's team, intense land use, encompassing agricultural activity and gravel mining, have devastated the river channel and the bordering floodplains. To this day, the corridor of the Eygues remains devoid of the riparian vegetation that once surrounded it. ■

Recommended research: Kondolf *et al.* (2007).

21.( ) Sarma and Acharjee (2018) reported a case study based on several years' worth of hydrologic data for the Brahmaputra River in India. They found that braiding in this body of water is intensified by factors such as its geologic composition – that is, the prevalence of erodible alluvial banks – and dramatic variations in discharge, even within a single day. Surprisingly, however, Sarma and his colleague found no relationship between the river reaches' braiding index and channel width.

Recommended research: Sarma and Acharjee (2018).

Theoretical analysis based on considerations of maximum flow efficiency (MFE) and the least action principle (LAP) indicates that, by developing anabranching planforms, rivers adjust so that maximum sediment-transport efficiency matches the prevailing supply of sediment without the need for changes in channel slope.

22.( ) This view is espoused in Tabata and Hickin (2003), who worked with the anastomosing channel system of the Columbia River in Canada. ■

Recommended research: Tabata and Hickin (2003).

Toffolon and Piccolroaz (2015) developed a simple model, named *air2stream*, to compute river water temperature. Their formulation was validated with data from three Swiss rivers characterized by different hydrological conditions. Further, the model is physically-based (which is to say that data inform the model without the need to rely on empirical formulations) and relies upon a large mass of geometric and hydraulic data.

23.( ) The most important feature of the Toffolon-Piccolroaz temperature model, arguably, is that is requires only daily values of air temperature and flow discharge, with no need for additional inputs. ■

Recommended research: Toffolon and Piccolroaz (2015).

Taylor's frozen turbulence hypothesis (FTH) holds that coherent turbulent structures remain unchanged as they pass by a measurement point, and that temporal lag of the structure can be scaled to its spatial extent using the local mean velocity.

24.( ) Rhoads and Sukhodolov (2004) studied the dynamics of the shear layer located in the confluence of Kaskaskia River and Copper Slough, East Central Illinois, and found that the FTH is not valid for that site, irrespective of eddy frequency or size. ■

Recommended research: Rhoads and Sukhodolov (2004)

Equipment used by Rhoads and Sukhodolov (2004).

Constantinescu *et al.* (2011) used an eddy-resolving simulation (DES) to study the three-dimensional structure of time-averaged and instantaneous flow at the same asymmetrical Illinois river confluence mentioned in the previous statement. They showed that the DES provides a more detailed description of the flow and turbulent structure in the confluence hydrodynamic zone than can be derived from field data. What's more, the DES easily captures coherent structures over the entire flow domain and allows for easy estimation of quantities that are difficult to measure in the field, such as bed friction velocity.

25.( ) Constantinescu's team went on to compare their DES with a Reynolds-averaged Navier-Stokes (RANS) scheme and found that the former afforded more accurate predictions of mean streamwise velocity and turbulent kinetic energy. ■

Recommended research: Constantinescu *et al.* (2011).

26.( ) Rhoads *et al.* (2009) studied the systematic response of bed morphology to hydrological variability and the extent of long-term change in channel morphology resulting from net hydrological conditions in the Kaskaskia-Cooper confluence (the same confluence mentioned in the previous two statements). The following illustrations are conceptual models for the spatial patterns of surficial bed material and bed morphology at the confluence in question; we can surmise that illustration **A** refers to conditions for high discharge ratio, whereas **B** describes conditions for low discharge ratio.

Recommended research: Rhoads *et al.* (2009).

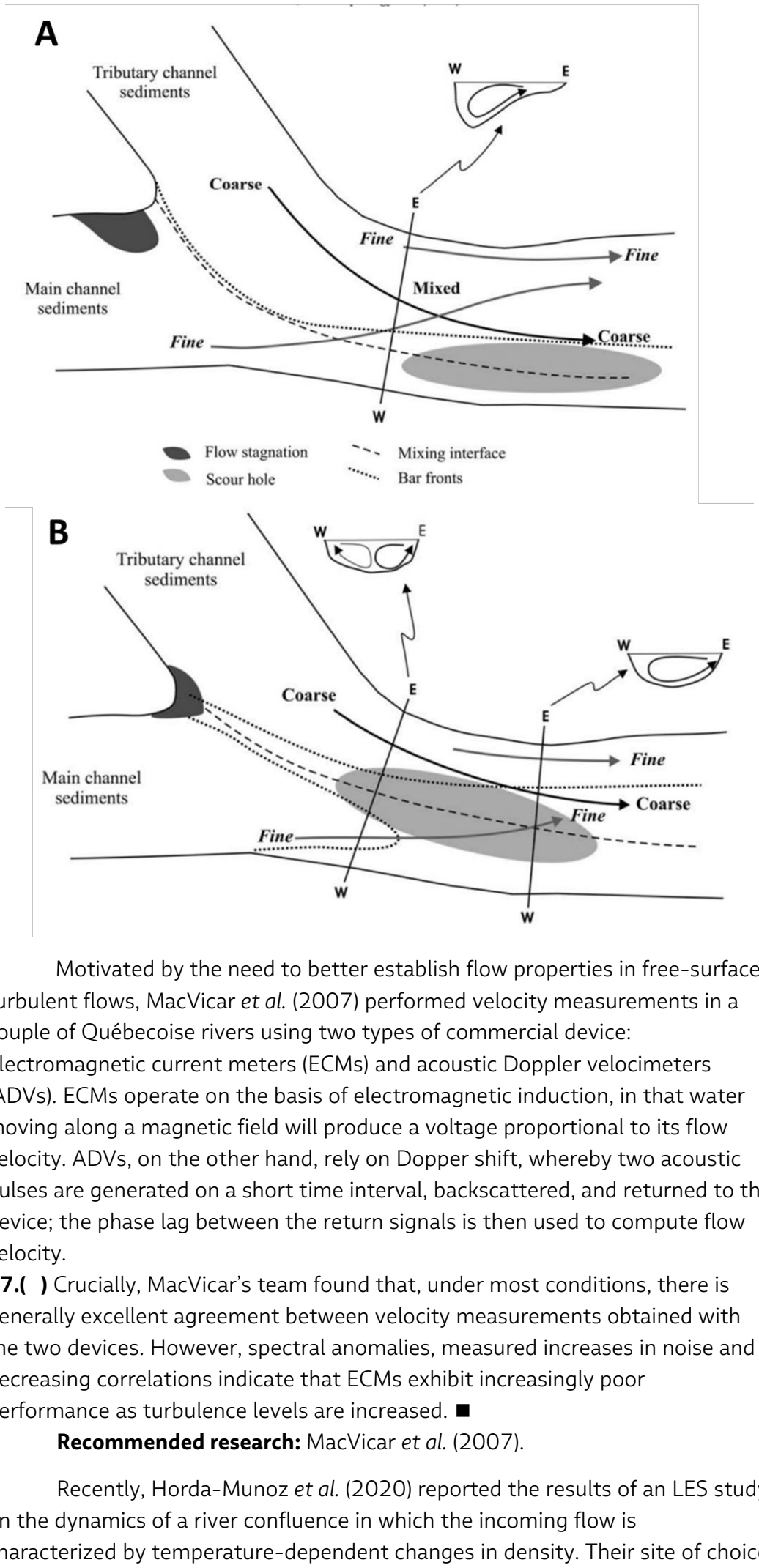

Motivated by the need to better establish flow properties in free-surface turbulent flows, MacVicar *et al.* (2007) performed velocity measurements in a couple of Québecoise rivers using two types of commercial device: Electromagnetic current meters (ECMs) and acoustic Doppler velocimeters (ADVs). ECMs operate on the basis of electromagnetic induction, in that water moving along a magnetic field will produce a voltage proportional to its flow velocity. ADVs, on the other hand, rely on Dopper shift, whereby two acoustic pulses are generated on a short time interval, backscattered, and returned to the device; the phase lag between the return signals is then used to compute flow velocity.

27.( ) Crucially, MacVicar's team found that, under most conditions, there is generally excellent agreement between velocity measurements obtained with the two devices. However, spectral anomalies, measured increases in noise and decreasing correlations indicate that ECMs exhibit increasingly poor performance as turbulence levels are increased. ■

Recommended research: MacVicar *et al.* (2007).

Recently, Horda-Munoz *et al.* (2020) reported the results of an LES study on the dynamics of a river confluence in which the incoming flow is characterized by temperature-dependent changes in density. Their site of choice with which to validate the model was, you guessed it, the Kaskaskia-Cooper confluence in Illinois.

In their paper, it is noted that although large-scale two-dimensional particle image velocimetry (PIV) has been used to improve characterization of surface flow structure at confluences, it is not nearly as useful when the structure of flow beneath the surface differs from the structure at the surface, so that surface observations will not shed light on subsurface patterns of mixing. On the other hand, Large Eddy Simulation (LES) may prove adequate as a method to obtain data with a sufficiently high 3D spatial resolution to

characterize the position, spatial extent, and coherence of the main vortical structures inside the confluence hydrodynamic zone (CHZ).

28.( ) In contrast to earlier work that had showed no occurrence of streamwise-oriented vortical (SOV) cells for certain Froude number values, Horda-Munoz's team reported that such cells were observed in every configuration of their numerical model. ■

Recommended research: Horda-Munoz *et al.* (2020).

Penna *et al.* (2018) studied the effects of varying junction angle on the flow structure of a confluence with fixed concordant beds and low width and discharge ratios. The angle α of the junction (see illustration below) was varied from 45 to 90°, and, in order to isolate the effect of angle changes, all else was kept constant.

29.( ) Penna's team found that, as the junction angle α increases, the retardation zone became increasingly narrower and shorter. In contrast, the length and width of the separation zone increased exponentially with α. ■

Recommended research: Penna *et al.* (2018).

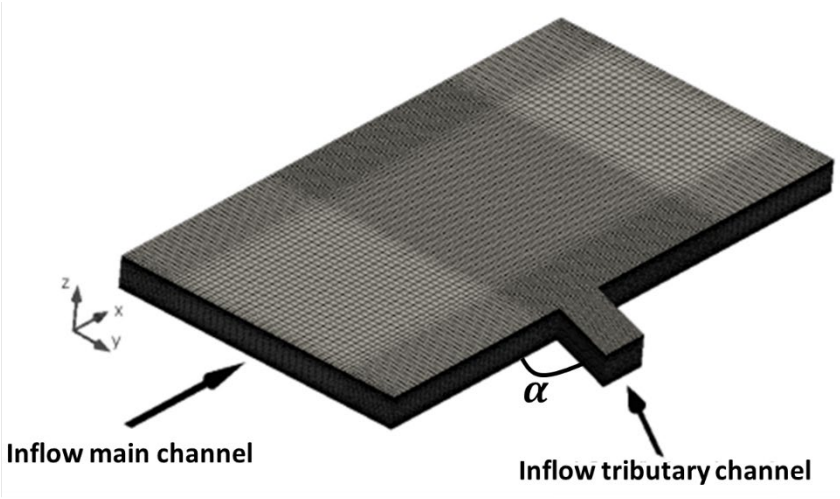

30.( ) Shakibainia *et al.* (2010) developed a three-dimensional numerical model to assess the dynamics of a typical river confluence. Their model emphasized the separation zone which is known to form in the inner wall of the post-confluence channel. Specifically, Shakibainia's team verified that the size of the separation zone increased with confluence angle and Froude number. On the other hand, the separation zone shrank for increasing discharge and width ratios.

Recommended research: Shakibainia *et al.* (2010).

31.( ) Guven and Howard (2006) developed a deterministic model to simulate the growth and movement of cyanobacterial blooms in river systems. Importantly, the main drawback of the Guven-Howard approach is that it requires river flow to be laminar; turbulent flow, with its inherent velocity fluctuations, could not be integrated into the model.

Recommended research: Guven and Howard (2006).

32.( ) The survival rate of a salmonid embryo in a running river stream is closely related to the size of the surrounding gravel sediment. The graph to the side relates percent embryo survival for a few salmonid species as a function of the ratio of gravel diameter to egg diameter. With reference to this graph, we see that the survival rate is greater for eggs surrounded by finer gravel than for eggs surrounded by coarser gravel.

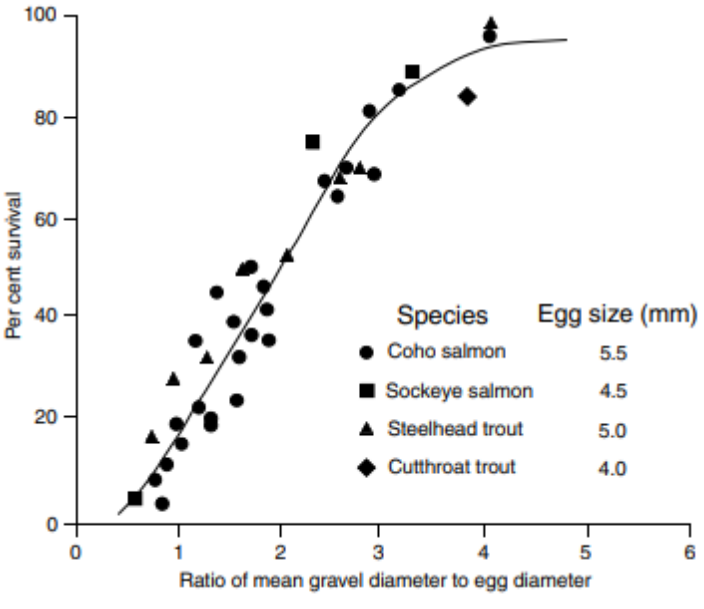

Sand-Jensen (2003) noted that, at the time of his writing, there were few studies on how submerged freshwater macrophytes adjusted themselves to minimize drag forces when exposed to rapid water flow, as in the case of streams and rivers. Accordingly, Sand-Jensen devised an experimental apparatus to assess the hydrodynamic response of five species of macrophytes, as illustrated below.

33.( ) Sand-Jensen found that there was a linear relationship between $\tan \phi$, where ϕ is the shoot angle of the plants relatively to the horizontal, and the velocity of water flow. Crucially, he found that this relationship applied to all five plant species and held throughout the entire set of velocities included in the test, indicating a consistent response of bending to increases in velocity. ■

Recommended research: Sand-Jensen (2003).

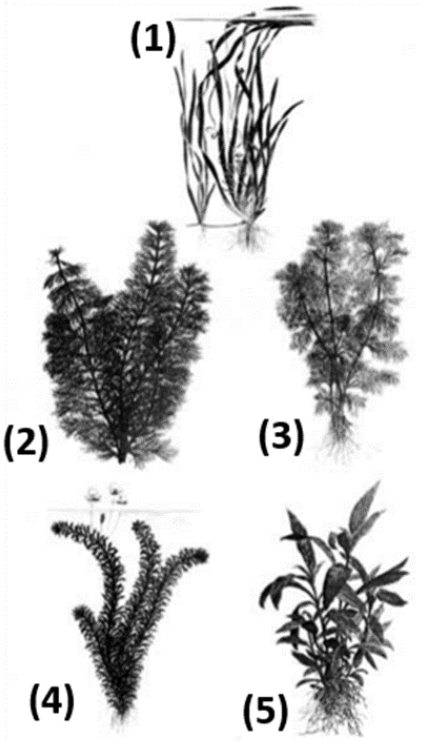

(1) *Vallisneria natans*
(2) *Limnophila aquatica*
(3) *Myriophyllum tuberculatum*
(4) *Egeria densa*
(5) *Hygrophila corymbosa*

Gippel (1995) reviewed the literature on the hydraulic effects of woody debris in rivers. A common problem in the management of debris in rivers is how to reconcile the need to maximize the volume of wood in the channel for ecological benefits and the concomitant need to minimize the volume of wood in the channel to lower flow resistance.

34.( ) Removal of debris is accompanied by reductions in flow resistance, which increases flow speed and thereby offers more feeding sites for fish. What's more, removal of debris may reduce overbank flooding and thereby afford better conditions for fish that depend on access to floodplain wetlands for spawning. ■

Recommended research: Gippel (1995).

The United Nations' Intergovernmental Panel on Climate Change (IPCC) has repeatedly warned that the climate crisis may severely disrupt fluvial dynamics across the world, leading to potentially catastrophic consequences; in the higher latitudes of the Northern Hemisphere, for instance, river discharge may sharply increase in spring due to early snow melting and increased winter precipitation.

35.( ) With these potential changes in mind, Masaki *et al.* (2014) used a hydrological model to assess seasonal inequality of river discharge under ongoing climate change. In doing so, they resorted to the Lorenz asymmetry coefficient (LAC), a coefficient originally employed to evaluate economic inequality among households; the LAC varies between 0 (inclusive) and 1 (inclusive). ■

Recommended research: Masaki *et al.* (2014).

▶ Problem 4

Associate the river water quality models with the corresponding definition.

1. SIMCAT (*Simulation catchment*)
2. TOMCAT (*Temporal overall model for catchments*)
3. QUAL2Kw
4. WASP8 (*Water quality analysis simulation program*)
5. QUASAR (*Quality simulation along rivers*)

P.( ) A free water quality and flow model for non-tidal rivers; can be run in *dynamic* and *planning* modes.
Q.( ) Offers no allowance for temporal variability and does not account for photosynthesis, respiration, or sediment oxygen demand.
R.( ) A one-dimensional model used mainly for a river's main stem, with no support for branching.
S.( ) Similar to SIMCAT, has been used in modelling orthophosphate concentrations in the river Thames.
T.( ) Developed by the US EPA, can be used for 1-, 2-, or 3D simulations.

SOLUTIONS

P.1 ➡ *Solution*

Per the Manning-Strickler approximation, $m = 1/6 \approx 0.167$. Substituting into the four given correlations brings to

$$h = 0.133 \times 200^{\frac{1}{3\times 0.167+2}} \times 0.028^{\frac{6\times 0.167-1}{6\times 0.167+4}} \times 0.05^{\frac{-1}{6\times 0.167+4}} = 2.01\,\text{m}$$

$$W = 0.512 \times 200^{\frac{2\times 0.167+1}{3\times 0.167+2}} \times 0.028^{\frac{-4\times 0.167-1}{6\times 0.167+4}} \times 0.05^{\frac{-2\times 0.167-1}{6\times 0.167+4}} = 63.3\,\text{m}$$

$$V = 14.7 \times 200^{\frac{0.167}{3\times 0.167+2}} \times 0.028^{\frac{2-2\times 0.167}{6\times 0.167+4}} \times 0.05^{\frac{2\times 0.167+2}{6\times 0.167+4}} = 1.57\,\text{m/s}$$

$$S = 12.4 \times 200^{3\times 0.167+2} \times 0.028^{6\times 0.167+4} \times 0.05^{6\times 0.167+4} = 0.00115$$

Using the value of h obtained above, we check the corresponding exponent m:

$$m = \frac{1}{2.3\log_{10}(2h/d_{50})} = \frac{1}{2.3\log_{10}(2\times 2.01/0.028)} = 0.202$$

There is considerable disagreement between this value and our assumed value of 0.167. We can proceed to update the four variables with the newly obtained $m = 0.202$ and check whether the new results yield a better agreement. A quicker way to proceed, however, is to equate

$$h \approx 0.133 \times 200^{\frac{1}{3m+2}} \times 0.028^{\frac{6m-1}{6m+4}} \times 0.05^{\frac{-1}{6m+4}}$$

and

$$\frac{1}{2.3\log_{10}(2h/0.028)}$$

and then solve the ensuing equation for h, using, for example, Mathematica's *FindRoot* command:

```
In[120]:= m = 1 / (2.3 * Log10[2 * h / 0.028]);

In[121]:= FindRoot[h - 0.133 * 200^(1/(3*m+2)) * 0.028^((6*m-1)/(6*m+4)) * 0.05^(-1/(6*m+4)), {h, 1}]

Out[121]=
          {h → 1.40711}
```

That is, $h \approx 1.41$ m. The corresponding value of m is

$$m = \frac{1}{2.3\log_{10}(2\times 1.41/0.028)} = 0.217$$

so that, substituting in the formulas for W, V, and S, we obtain

$$W = 0.512 \times 200^{\frac{2\times0.217+1}{3\times0.217+2}} \times 0.028^{\frac{-4\times0.217-1}{6\times0.217+4}} \times 0.05^{\frac{-2\times0.217-1}{6\times0.217+4}} = \underline{71.3\,\text{m}}$$

$$V = 14.7 \times 200^{\frac{0.217}{3\times0.217+2}} \times 0.028^{\frac{2-2\times0.217}{6\times0.217+4}} \times 0.05^{\frac{2\times0.217+2}{6\times0.217+4}} = \underline{1.99\,\text{m/s}}$$

$$S = 12.4 \times 200^{\frac{-1}{3\times0.217+2}} \times 0.028^{\frac{5}{6\times0.217+4}} \times 0.05^{\frac{6\times0.217+5}{6\times0.217+4}} = \underline{0.00164}$$

In summary, the river should have a surface width of about 71 meters, a flow depth of about 1.4 meters, a flow velocity of about 2 meters per second, and a friction slope of about 0.0016.

P.2 ➡ *Solution*

The maximum deviation angle can be found with the simple relation

$$R_m = \frac{L}{2\pi\theta_m} \rightarrow \theta_m = \frac{L}{2\pi R_m}$$

$$\therefore \theta_m = \frac{500}{2\pi \times 83} = 0.960\,\text{rad} = \boxed{54.9^\text{o}}$$

Noting that $J_0()$ denotes a Bessel function of first kind and order zero, the meander length Λ is found as

$$\Lambda = LJ_0\left(\theta_m\right) = 500 \times J_0\left(0.960\right) = \boxed{391\,\text{m}}$$

Then, the sinuosity Ω follows as

$$\Omega \equiv \frac{L}{\Lambda} = \frac{500}{391} = \boxed{1.28}$$

It remains to compute the meander width W_n,

$$W_m = \frac{L}{2} H_0\left(\theta_m\right) = \frac{500}{2} \times H_0\left(0.960\right) = \boxed{138\,\text{m}}$$

where $H_0()$ denotes a Struve function of order zero.

P.3 ➡ *Solution*

1.True. The main regression equation obtained by Williams is

$$Q_b = 4.0 A_b^{1.81} S^{0.28}$$

where Q_b is bank-full discharge in cubic meters per second, A_b is bank-full cross-sectional area in squared meters, and S is longitudinal slope. Note that bank-full depth D_b is nowhere to be seen in this equation. Williams' regression analysis, run at a probability level of 0.05, found D_b and roughness variables to not be statistically significant.

Reference: Williams (1978).

2.False. The opposite is correct, in that Parker (1979) found good consistency between the exponents but high disagreement in the pre-exponential coefficients. More scrutiny of power-law hydraulic geometry theory has indicated further shortcomings of this approach, including, for instance, the fact that exponent values for high-flow conditions can be very different from those obtained for low-flow conditions within the same site.

References: Singh (2003); Parker (1979).

3.False. Yang's analysis relied on the Manning-Strickler formula and was limited to self-formed channels whose shape can be approximated by rectangles.

Reference: Yang *et al.* (1981).

4.True. Indeed, in the PCA conducted by Oueslati *et al.* (2015), perennial rivers were mostly linked to high-flow condition indices (e.g., those indicating the magnitude of flow during wet months), whereas temporary streams were markedly linked to indices associated with zero-flow days, predictability of flow, and flow variability.

Reference: Oueslati *et al.* (2015).

5.False. A steep mountain torrent or a glacial outwash stream is expected to have a much greater fining rate than a lowland sand-bed river.

6.False. Much to the contrary, Ferguson (2005) corrected Bagnold's stream power equation to a form that uses only readily available channel properties. Specifically, Ferguson made a simple adjustment to express critical stream power in terms of channel gradient – a control of depth – instead of flow depth itself.

Reference: Ferguson (2005).

7.True. For constant discharge and sediment load, and an exponential decrease in particle size over distance, a typical numerical model will indicate that sand-bed rivers may delineate straight or slightly concave-upward profiles, whereas gravel-bed rivers will have concave-upward profiles. Accordingly, changes in the size of bed material have a stronger influence on profile concavity in gravel-bed rivers than in sand-bed rivers, assuming that abundant amounts of material are in transport.

Reference: Rhoads (2020).

8.False. Noting that his bank erosion coefficient was expected to be a function of bank soil properties only, Hasegawa (1989) resorted to a parameter that was readily available in the Hokkaido rivers he worked with: the number N of blows obtained in the standard penetration test (SPT). It is important to know the deepest layer to which the river in question is capable of scouring; in view of this necessity, Hasegawa went on to characterize the bank material relatively to the value N_D of the SPT, where N_D represents the spatial mean of the N values as measured downward from the exposed upper bank edge to the depth of deepest scour.

Reference: Hasegawa (1989).

9.False. The final parts of the statement are precisely aspects of turbulent fluvial dynamics that Roy's model does *not* cover.

Reference: Roy *et al.* (2004).

10.False. Shvidchenko and Pender (2001) actually found that the longitudinal size of the eddies was around 4 to 5 flow depths on average, whereas the transversal size was about 2 depths.

Reference: Shvidchenko and Pender (2001).

11.True. MacDonald's team reported appreciable disagreement between measured data and numerical simulation near the base of the plume, noting that one explanation could be the existence of small-scale heterogeneity in the turbulent field at that region, which their numerical scheme may have failed to capture.

Reference: MacDonald *et al.* (2007).

12.True. Indeed, the experiments by Rodríguez and García (2008), which included $b/h = 8.5$ and $b/h = 6.3$, exhibited clear secondary circulation patterns even though the rule mentioned in the statement would predict weak or inexistent secondary circulation patterns in the central region of the channel.

Reference: Rodríguez and García (2008).

13.False. In actuality, Franca and Lemmin observed that ejections had a shorter duration than sweeps, as they covered only 35% of a LSFS cycle.

Reference: Franca and Lemmin (2015).

14.False. Chen and Duan (2006) actually adopted four formulations for A. In the first, $A = 2.0$; in the second, $A = t/60$, that is, the parameter varies linearly with time; in the third, $A = (t/30)^{1/2}$, that is, A evolves with the square root of time; in the fourth, $A = t^2/7200$, that is, A evolves with time squared. Chen and his colleague found that the channel migrated downstream too rapidly when the parameter A was defined by either the second or the fourth approaches; on the other hand, the channel migrated too slowly when A was assumed to be a constant. Accordingly, Chen and Duan ultimately opted for the third approach.

Reference: Chen and Duan (2006).

15.True. Total sinuosity of braiding increases with increasing potential bankfull stream power per unit length of channel and with decreasing grain size of bed material. Likewise, the braiding index increases with stream power.

16.False. The simulations of Sun *et al.* (1996) were actually two-dimensional in nature.

Reference: Sun *et al.* (1996).

17.False. On the contrary, Lancaster and Bras (2002) found that, in their model, compound bend formation is relatively insensitive to changes in valley slope S_v and grain size d_{50}.

Reference: Lancaster and Bras (2002).

18.True. This is indeed correct. Zinger *et al.* (2011) conclude that chute cutoff events have the potential to perform geomorphic work at extreme rates by releasing large pulses of sediment into river channels from adjacent floodplains. It follows that chute cutoffs may be an important, albeit until then rarely recognized, mechanism of sediment delivery to meandering rivers.

Reference: Zinger *et al.* (2011).

19.True. Indeed, Wrzesinski (2016) reports that low entropy values, mostly under 1.0 bit, were indicative of high certainty in monthly river runoff and occurred mostly in lakeland rivers and on lowland rivers in the northern part of the country; on the other hand, the highest entropies of monthly runoff, exceeding 2.5 bits, were generally associated with mountain rivers.

Reference: Wrzesinski (2016).

20.True. In spite of intense activity, the riparian forest surrounding the Eygues saw a resurgence in the years leading to the Kondolf *et al.* (2007) paper. As the channel recovered from the high sediment loads and intense agricultural use of riparian lands, the riparian forest spontaneously reestablished itself on active channel area. However, the active nature of the channel means that the riparian forest is frequently disturbed, and succession interrupted, such that the riparian forest is dominated by pioneer and mid-successional stage stands, in lieu of the later-successional-state species that had once prevailed in the area.

Reference: Kondolf *et al.* (2007).

21.False. Sarma and Acharjee (2018) note that most rivers will braid when channel width surpasses 60 times the depth. For some sections of the Brahmaputra, this ratio is as large as 800, indicating that some sections of the river are in fact susceptible to braiding. Indeed, Sarma and his colleague reported a positive correlation between river width and braiding index.

Reference: Sarma and Acharjee (2018).

22.False. Much to the contrary, Tabata and Hickin (2003) argue that, in their Canadian case study at least, a river in a slope-constrained environment does not necessarily develop anabranching patterns as a means to achieve greater hydraulic efficiency.

Reference: Tabata and Hickin (2003).

23.True. Indeed, Toffolon and Piccolroaz (2015) developed a model that affords temperature values on the basis of temperature and flow discharge only, which, they argued, makes *air2stream* superior to standard mechanistic models, which would require additional inputs that are often unavailable. *air2stream* performs well without the need to consider local shading, cloud cover, atmospheric influences, or the temporal variability of the various forcings.

Reference: Toffolon and Piccolroaz (2015).

24.False. Rhoads and Sukholodov (2004) note that, in a typical confluence shear layer, complex patterns of vortex growth, interaction and amalgamation may produce hydrodynamic conditions that do not conform to the frozen-turbulence hypothesis. Still, those workers verified that the FTH holds for the Kaskaskia-Copper confluence for frequencies greater than 0.3 Hz and separation distances of approximately 1.5 m. This domain includes the frequencies greater than 0.75 Hz where turbulence is isotropic and power law scaling between turbulence energy and frequency holds. In other words, the range of frequencies greater than 0.75 Hz conforms to the inertial subrange characterized by a smooth cascade of turbulence energy. Between 0.3 and 0.75

Hz the power spectra of streamwise and transverse velocity fluctuations overlap and exceed the spectrum for vertical velocity. Thus, the frozen turbulence hypothesis holds for a portion of the frequency range corresponding to quasi-two-dimensional turbulence characterized by coherent rotating structures generated via Kelvin-Helmholtz-like instability of the shear layer.

Reference: Rhoads and Sukholodov (2004).

25.True. Constantinescu *et al.* (2011) note that the main reason for the poor level of agreement of the RANS simulation with the measured data is the substantial underprediction of the coherence and circulation of streamwise-oriented vertical (SOV) cells.

Reference: Constantinescu *et al.* (2011).

26.True. The alignment of the scour hole tracks changes in the location of the mixing interface between the converging flows. During high-discharge-ratio events, flow and sediment from the Cooper Slough penetrate far into the confluence and the mixing interface extends from the junction apex toward the outer bank. Under low-discharge-ratio conditions, the mixing interface is located near the center of the confluence and downstream channel. Accordingly, Rhoads *et al.* (2009) note that scour is confined to the outer bank during high-discharge-ratio events (illustration A), but it is located close to the center of the confluence and downstream channel during low-discharge-ratio conditions (illustration B).

Reference: Rhoads *et al.* (2009).

27.False. The statement would've been correct if, in the last sentence, we'd replaced 'ECMs' with 'ADVs'. ADVs are non-intrusive, do not require calibration and measure at higher frequencies; these factors have led to widespread adoption of this type of device. But spectral anomalies and measured increases in noise from the power spectra indicate that ADV error grows as a result of intensified turbulence, particularly for the vertical velocity component.

Reference: MacVicar *et al.* (2007).

28.True. Indeed, Horda-Munoz's team found that SOV cells occurred in all settings they tested. Density contrasts between the incoming flows influence the position, length, and degree of coherence of the different SOV cells and can generate SOV cells that do not exist in the corresponding no-density-effects case.

Reference: Horda-Munoz *et al.* (2020).

29.False. In actuality, Penna *et al.* (2018) found that, with increasing α, the degree of flow retardation increased near the upstream lateral bank of the tributary channel, implying a wider and longer retardation zone and a lower velocity in this region. Further, it was verified that increasing α led to a longer and wider separation zone, but the observed trend was linear, not exponential.

Reference: Penna *et al.* (2018).

30.True. Part of this statement is taken verbatim from the conclusion of the Tatabai *et al.* (2010) paper. Indeed, those workers' simulations with the SSIIM2.0 code showed that an increase in the confluence angle and Froude number, or a decrease in the discharge and width ratios, led to a larger separation zone; a narrower contraction zone with the higher velocity, stronger and more distinguishable helical cells; and intensified water surface variations in the confluence.

Reference: Shakibainia *et al.* (2010).

31.False. Much to the contrary, the hydraulic component (or 'sub-model', as they put it) of the model proposed by Guven and Howard (2006) does in fact account for colony motion under both laminar and turbulent flows. The following graph shows the depth *uersus* distance (along the reach) achieved by the cyanobacterial colonies; the solid and coarse lines refer to colony movement under turbulent and laminar flow, respectively; as can be seen, the vertical velocities of the colonies are higher in turbulent environments.

Reference: Guven and Howard (2006).

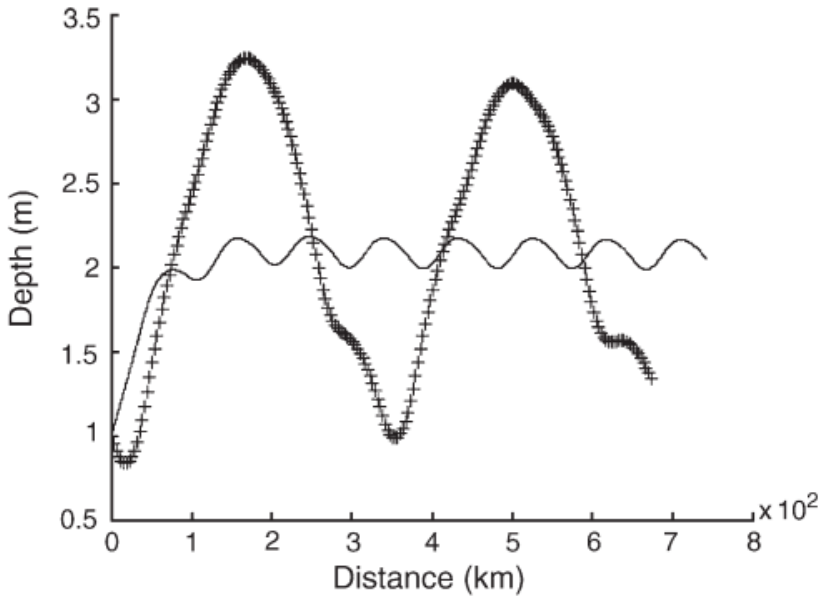

32.True. This is a simple observational exercise: the curve rises monotonically as the abscissae increase, indicating that survival rates are greater for eggs surrounded by finer gravel or, equivalently, for larger eggs. Of course, an egg's odds of survival in a running stream are also related to other conditions, such as the availability of interstitial voids and an adequate supply of oxygen.

33.False. The statement errs twice. Firstly, Sand-Jensen (2003) found a linear relationship between $log(tan\ \phi)$ and velocity, not $tan\ \phi$ itself. Secondly, he found that the negative linear relationship in question was only valid up to a certain velocity level, as speeds beyond 50 cm/s elicited no significant additional bending in all but one of the five plant species. Sand-Jensen suggested that there may be a threshold velocity level beyond which "further compression of the shoots is counteracted by insufficient elasticity of the stem and/or dense packing of shoots in a diminishing water volume."

Reference: Sand-Jensen (2003).

34.False. Gippel (1995) notes that the best feeding sites for fish are low-velocity zones adjacent to higher-velocity flows or eddies, which provide a concentrated source of food. It follows that the faster flow afforded by removal of woody debris may not aid fish survival at all. Likewise, decreased flooding can seriously impact fish species that require seasonal access to floodplain wetlands for spawning and use as a nursery habitat.

Reference: Gippel (1995).

35.False. The final sentences of the statement actually describe the Gini coefficient, not the Lorenz asymmetry factor. The Gini coefficient, G, was proposed as a measure of inequality in the distribution of income, wealth, or resources among members (not necessarily individuals but also families, cities or nations). Its value varies between zero and 1. In the hydrological context of Masaki *et al.* (2014), a $G = 0$ implies that there is complete equality (constant discharge throughout the year without any seasonal variation), whereas $G = 1$ implies that the annual amount of discharge of a river occurs at a single instance and there is no flow for the rest of the year.

Reference: Masaki *et al.* (2014).

P.4 ➡ *Solution*

The correct associations are tabulated below.

P	Q	R	S	T
5	1	3	2	4

REFERENCES

- Chen, D. and Duan, J.G. (2006). Modeling width adjustment in meandering channels. *J Hydrol*, 321(1 – 4), 59 – 76. DOI: 10.1016/j.jhydrol.2005.07.034
- Constantinescu, G., Miyawaki, S., Rhoads, B. *et al.* (2011). Structure of turbulent flow at a river confluence with momentum and velocity ratios close to 1: Insight provided by an eddy-resolving numerical simulation. *Water Resour Res*, 47, W05507. DOI: 10.1029/2010WR010018

- DINGMAN, S.L. (2009). *Fluvial Hydraulics*. Oxford: Oxford University Press.
- Ferguson, R.I. (2005). Estimating critical stream power for bedload transport calculations in gravel-bed rivers. *Geomorphology*, 70(1 – 2), 33 – 41. DOI: 10.1016/j.geomorph.2005.03.009
- Franca, M.J. and Lemmin, U. (2014). Detection and reconstruction of large-scale coherent flow structures in gravel-bed rivers. *Earth Surf Process Landforms*, 40, 93 – 104. DOI: 10.1002/esp.3626
- Gippel, C.J. (1995). Environmental hydraulics of large woody debris in streams and rivers. *J Environ Eng*, 121(5), 388 – 395. DOI: 10.1061/(ASCE)0733-9372(1995)121:5(388)
- Guven, B. and Howard, A. (2006). Modelling the growth and movement of cyanobacteria in river systems. *Sci Total Environ*, 368(2 – 3), 898 – 908. DOI: 10.1016/j.scitotenv.2006.03.035
- Hardy, R.J., Best, J.L., Lane, S.N. *et al.* (2009). Coherent flow structures in a depth-limited flow over a gravel surface: The role of near-bed turbulence and influence of Reynolds number. *J Geophys Res*, 114, F01003. DOI: 10.1029/2007JF000970
- Hasegawa, K. (1989). Universal bank erosion coefficient for meandering rivers. *J Hydraul Res*, 115(6), 744 – 765. DOI: 10.1061/(ASCE)0733-9429(1989)115:6(744)
- Horda-Munoz, D., Constantinescu, G., Rhoads, B. *et al.* (2020). Density effects at a concordant bed natural river confluence. *Water Resour Res*, 56, e2019WR026217. DOI: 10.1029/2019WR026217
- JULIEN, P.Y. (2018). *River Mechanics*. 2nd edition. Cambridge: Cambridge University Press.
- Julien, P.Y. and Wargadalam, J. (1995). Alluvial channel geometry: Theory and applications. *J Hydraul Eng*, 121(4), 312 – 325. DOI: 10.1061/(ASCE)0733-9429(1995)121:4(312)
- KONDOLF, G.M. and PIÉGAY, H. (Eds.) (2016). *Tools in Fluvial Geomorphology*. 2nd edition. Oxford: Wiley-Blackwell.
- Kondolf, G.M., Piégay, H. and Landon, N. (2007). Changes in the riparian zone of the lower Eygues River, France, since 1830. *Landscape Ecol*, 22, 367 – 384. DOI: 10.1007/s10980-006-9033-y
- Lancaster, S.T. and Bras, R.L. (2002). A simple model of river meandering and its comparison to natural channels. *Hydrol Process*, 16, 1 – 26. DOI: 10.1002/hyp.273
- MacDonald, D.G., Goodman, L. and Hetland, R.D. (2007). Turbulent dissipation in a near-field river plume: A comparison of control volume and microstructure observations with a numerical model. *J Geophys Res*, 112, C07026. DOI: 10.1029/2006JC004075
- MacVicar, B.J., Beaulieu, E., Champagne, V. *et al.* (2007). Measuring water velocity in highly turbulent flows: field tests of an electromagnetic current meter (ECM) and an acoustic Doppler velocimeter. *Earth Surf Process Landforms*, 32, 1412 – 1432. DOI: 10.1002/esp.1497
- Masaki, Y., Hanasaki, N., Takahashi, K. *et al.* (2014). Global-scale analysis on future changes in flow regimes using Gini and Lorenz asymmetry coefficients. *Water Resour Res*, 50, 4054 – 4078. DOI: 10.1002/2013WR014266
- Oueslati, O., de Girolamo, A.M., Abouabdillah, A. *et al.* (2015). Classifying the flow regimes of Mediterranean streams using multivariate analysis. *Hydrol Process*, 29, 4666 – 4682. DOI: 10.1002/hyp.10530
- Parker, G. (1979). Hydraulic geometry of active gravel rivers. *J Hydraul Div*, 105(9), 1185 – 1201. DOI: 10.1061/JYCEAJ.0005275
- Penna, N., de Marchis, M., Canelas, O.B. *et al.* (2018). Effect of the junction angle on turbulent flow at a hydraulic confluence. *Water*, 10(4), 469. DOI: 10.3390/w10040469
- RHOADS, B.L. (2020). *River Dynamics*. Cambridge: Cambridge University Press.
- Rhoads, B.L. and Sukhodolov, A.N. (2004). Spatial and temporal structure of shear layer turbulence at a stream confluence. *Water Resour Res*, 40, W06304. DOI: 10.1029/2003WR002811
- Rhoads, B.L., Riley, J.D. and Mayer, D.R. (2009). Response of bed morphology and bed material texture to hydrological conditions at an

asymmetrical stream confluence. *Geomorphology*, 109(3 – 4), 161 – 173. DOI: 10.1016/j.geomorph.2009.02.029

- Rodríguez, J.F. and García, M.H. (2008). Laboratory measurements of 3-D flow patterns and turbulence in straight open channel with rough bed. *J Hydraul Res*, 46(4), 454 – 465. DOI: 10.3826/jhr.2008.2994
- Roy, A.G., Buffin-Bélanger, T., Lamarre, H. *et al.* (2004). Size, shape and dynamics of large-scale turbulent flow structures in a gravel-bed river. *J Fluid Mech*, 500, 1 – 27. DOI: 10.1017/S0022112003006396
- Sand-Jensen, K. (2003). Drag and reconfiguration of freshwater macrophytes. *Freshw Biol*, 48, 271 – 283. DOI: 10.1046/j.1365-2427.2003.00998.x
- Sarma, J.N. and Acharjee, S. (2018). A study on variation in channel width and braiding intensity of the Brahmaputra River in Assam, India. *Geosciences*, 8(9), 343. DOI: 10.3390/geosciences8090343
- Shakibainia, A., Tabatabai, M.R.M. and Zarrati, A.R. (2010). Three-dimensional numerical study of flow structure in channel confluences. *Can J Civ Eng*, 37, 772 – 781. DOI: 10.1139/L10-016
- Shvidchenko, A.B. and Pender, G. (2001). Macroturbulent structure of open-channel flow over gravel beds. 37(3), 709 – 719. DOI: 10.1029/2000WR900280
- Singh, V.P. (2003). On the theories of hydraulic geometry. *Int J Sediment Res*, 18(3), 196 – 218.
- Sun, T., Meakin, P. and Jøssang, T. et al. (1996). A simulation model for meandering rivers. *Water Resour Res*, 32(9), 2937 – 2954. DOI: 10.1029/96WR00998
- Tabata, K.K. and Hickin, E.J. (2003). Interchannel hydraulic geometry and hydraulic efficiency of the anastomosing Columbia River, southeastern British Columbia, Canada. *Earth Surf Process Landforms*, 28, 837 – 852. DOI: 10.1002/esp.497
- Toffolon, M. and Piccolroaz, S. (2015). A hybrid model for river water temperature as a function of air temperature and discharge. *Environ Res Lett*, 10, 114011. DOI: 10.1088/1748-9326/10/11/114011
- Williams, G.P. (1978). Bank-full discharge of rivers. *Water Resour Res*, 14(6), 1141 – 1154. DOI: 10.1029/WR014i006p01141
- Wrzesinski, D. Use of entropy in the assessment of uncertainty of river runoff regime in Poland. *Acta Geophys*, 64, 1825 – 1839. DOI: 10.1515/acgeo-2016-0073
- Yang, C.T., Song, C.C.S. and Woldenberg, M.J. (1981). Hydraulic geometry and minimum rate of energy dissipation. *Water Resour Res*, 17(4), 1014 – 1018. DOI: 10.1029/WR017i004p01014
- Zinger, J.A., Rhoads, B.L. and Best, J.L. (2011). Extreme sediment pulses generated by bend cutoffs along a large meandering river. *Nature Geosci*, 4, 675 – 678. DOI: 10.1038/ngeo1260